Kufa Journal of Engineering
Vol. 8, No. 2, June 2017, P.P.1-17
Received 28 August 2016, accepted 6 November 2016

FINITE ELEMENT SIMULATION OF PLUGGED OPEN ENDED PILE BEHAVIOR

Mohammed Y. Fattah[1], Nahla M. Salim[2] and Asaad M. B. Al-Gharrawi[3]

[1] Professor, Building and Construction Engineering Department, University of Technology, Baghdad, Iraq, Email: myf_1968@yahoo.com

[2] Assistant Professor, Building and Construction Engineering Department, University of Technology, Baghdad, Iraq.

[3] Lecturer, Civil Engineering Department, University of Kufa, Iraq, Email: zfs_n@yahoo.com

ABSTRACT

Open-ended steel pipe piles are widely used for foundations both on land and offshore because of low cost compare with other types of piles and it does not need a high effort for driving. During driving process of these piles into the soil, a soil column known as the soil plug is formed inside the pile. As the penetration continues, the frictional resistance between the inner pile shaft and the soil plug may be developed and in turn may prevent further soil intrusion. Depending on the relative movement between the pile and the soil plug, the pile is considered to be perfectly plugged, imperfectly plugged or unplugged.

A numerical modeling of experiments was carried out using PLAXIS-2015 software, in which the Hardening Soil Model (HS small) has been used for soil modeling. During the verification problem used to simulate the experimental results of the pile group G2(2x2), the piles simulated as volume piles and steel cap were modeled using linear elastic model. The simulation showed that the maximum percentage of deviation between experimental and theoretical results is not more than 13.0%. This ratio is considered good when compared to the actual results and the theoretical results with the same values in some of the results.

KEYWORDS: Pipe pile, open-ended, fully plugged, finite elements, simulation.

محاكاة بطريقة العناصر المحددة لسلوك الركائز مفتوحة النهايات ذات السدادة

أ. د. محمد يوسف فتاح — **قسم هندسة البناء والانشاءات/ الجامعة التكنولوجية**

أ.م. د. نهلة محمد نوري سالم — **قسم هندسة البناء والانشاءات/ الجامعة التكنولوجية**

م. د. اسعد محمد باقر — **قسم الهندسة المدنية/ جامعة الكوفة**

الخلاصة:

تعتبر الركائز الأنبوبية الحديدية مفتوحة النهايات واسعة الاستعمال في الأسس عند اليابسة و في المنشآت البحرية وذلك لأنها رخيصة الثمن مقارنه بأنواع الركائز الاخرى ولا تحتاج الى جهد عالي عند تنفيذها. أثناء عملية الغرز لهذه الركائز في التربة يتكون عمود من التربة يعرف بسدادة التربة، و مع استمرار اختراق الركيزة يمكن أن تتنامى مقاومة الاحتكاك بين السطح الداخلي للركيزة و سدادة التربة مما ينتج عنه منع دخول مزيد من التربة. و اعتمادا على الحركة النسبية بين الركيزة و سدادة التربة تعتبر الركيزة إما مغلقة بشكل تام أو مغلقة بشكل غير تام أو غير مغلقة.

تم إجراء تمثيل عددي لتجارب عملية باستعمال برنامج الحاسبة PLAXIS-2015 حيث تم استعمال نموذج تصلب التربة HARDENING SOIL MODEL (HS SMALL) لتمثيل التربة. و خلال مسألة التحقق التي استعملت لمحاكاة النتائج العملية لمجموعة ركائز مؤلفة من (2 X 2) ركيزة باستعمال البرنامج PLAXIS-2015، حيث تم تمثيل الركائز كركائز حجمية و تمثيل قبعة الركائز الخرسانية باستعمال نموذج مرن خطي. لقد بينت المحاكاة أن نسبة الانحراف العظمى بين النتائج العملية و النظرية لا تزيد عن 13%.

1. INTRODUCTION

After an open-ended pile is driven into the ground, a soil plug may progress within the pile during driving, which may avoid or partially constrain additional soil from incoming the pile. It is known that the driving resistance and the bearing capacity of open-ended piles are administered to a large extent by this plugging effect. The design principles for open-ended piles, depend on field tests, chamber tests or systematic methods, have been studied, (Klos and Tejchman, 1977; American Petroleum Institute, API-1991; Randolph et al., 1991; Jardine et al., 1998). These principles are usually used for offshore foundation design, the bearing capacity of an open-ended pile able only be appreciation for either the completely coring mode or the fully plugged style of breakthrough.

Formation of a soil plug in an open-ended pile is a very important factor in determining pile behavior both during driving and during static loading. Most open-ended piles drive in coring mode but are plugged during static loading. On some occasions, piles may plug and impede driving. If the available pile hammer cannot drive the pile to the design depth, a problem may arise, particularly for piles with thickened walls near the surface or mud line, such as piles used to resist lateral loading (Murff et al., 1990). The formation of a soil plug in an open-ended pile is a very important factor in determining pile behavior both during driving and during static loading. The degree of soil plugging can be represented by the incremental filling ratio, defined as (Iskander, 2010).

Paikowsky and Whitman (1990) investigated the effect of soil plugging on the axial resistance developed by open-ended (pipe) piles installed in sand and clay. They described the process of soil plug formation during the initial stages of pile installation, the length of the soil plug (Lp) inside the pipe equals the pile penetration depth (L), and the pile is said to be coring (IFR =100%). As the pile penetration depth increases, frictional stresses between the inside wall of the pile and the soil plug may cause partial plugging (0% > IFR, 100%), and in some cases the pile may become completely plugged (IFR = 0%). They noted that plugging resulted in a large increase in the axial resistance of piles installed in sand and caused a large increase in the zone of excess pore water pressure surrounding piles in clay, causing a delay .The development of the soil core during installation is quantified by the plug length ratio (PLR) as equation (1) or the incremental filling ratio (IFR) in equation (2):

$$\text{PLR} = \frac{L\text{p}}{L} \tag{1}$$

$$\text{IFR} = \frac{\Delta L\text{p}}{\Delta L} \tag{2}$$

Paik and Salgado (2003) tested a model pile made of two very smooth stainless steel pipes with different diameters. It had an outside diameter of 42.7 mm, an inside diameter of 36.5 mm, and a length of 908 mm. Paik and Salgado explained the relationship between the plug length ratio (PLR) and IFR for the chamber calibration test, and it can be expressed as follows in equation (3):

$$IFR\% = 109PLR - 22 \tag{3}$$

2. BASE LOAD CAPACITY OF AN OPEN TUBULAR PILE

A small introduction to the basic load bearing capacity of an open tubular pile seems in place. The basic load-bearing capacity of an open tubular pile is composed of the tip resistance under the ring-shaped tip the pile and the internal friction in the post, which is generated by the soil which enters the post during the installation. The last of these two components is commonly referred to as the load bearing capacity of the soil plug. On this basis, the following formulation base load-bearing capacity is given as follows in equation (4):

$$\mathrm{Q_b} = \mathrm{Q_{ann}} + \mathrm{Q_{plug}} \tag{4}$$

where:

Q_b= base load capacity of the pile,

Q_{ann}= point resistance of the pile, and

Q_{plug}= bearing capacity of the soil plug in the pile.

In comparison with the closed tubular pile, the open tubular pile is not to be simply divided at the ground displacement piles. An open tubular pile implies less land displacement because penetrates during the installation floor and there are so constitutes a fundamental pillar in the post, namely the soil plug. This proposition is confirmed by the comparison of the radial stress generated by a closed tube pole and open tubular pile as shown in Fig. 1 (White and Bolton, 2005).

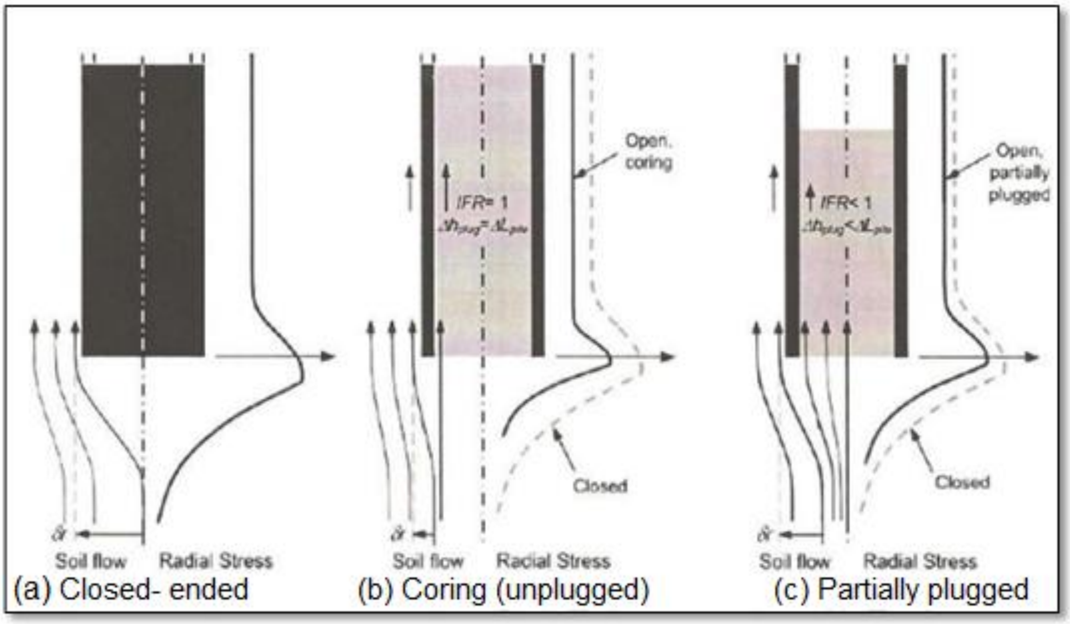

Fig. 1. Basic streamlining and radial stress (White and Bolton, 2005).

It is clear in Fig. 1- b situation, namely, an open tubular pile without plug formation, less soil displacement brings than c situation where the open tubular pile has already been partially plugged. These higher ground displacements logically also brings greater radial tensions. There is therefore provided that, as shown in field trials (Kishida, 1967; Paik et al., 2003), laboratory tests in test chambers (O'Neill and Raines, 1991; Foray et al., 1998, Fattah et al., 2016), and centrifuge tests on model piles and open tubular pile a reaction brings about that is located between those of a pile and a soil displacement drilled pile.

The objectives of this paper is to offer a better realization regarding the performance of pipe pile group under vertical loading with soil plug, and to provide valuable geotechnical data and parameters necessary for the numerical simulations and foundation design.

3. NUMERICAL MODELING OF PIPE PILES

The methods of analysis, which use the finite element technique, will be discussed in this study. The finite element method represents one of the extensive proliferation techniques in the representation of engineering applications (PLAXIS Manual, 2015). The review of equations that are concerned with the program of Plaxis-3D (2015) and how to build mathematical models depending on the soil type also will be discussed with details in this study. It also includes a verification process for the case of group piles (4-piles) driven in sandy soil and tested by the laboratory model. After fixing the soil properties in the theoretical model through the verification, which will be explained in this study. Full numerical analysis approach, attempts are made to satisfy all theoretical requirements, including realistic soil constitutive models and boundary conditions that realistically simulate field conditions. Approaches based on finite difference, boundary element and finite element methods are those most widely used. These methods essentially involve computer simulation of the history of the boundary value problem from field conditions, through construction in the long term. Their ability to reflect accurately the field conditions essentially depends on the ability of the constitutive model to represent real soil behavior and correctness of the boundary conditions imposed (PLAXIS Manual, 2015).

4. PLAXIS- 3D 2015 SOFTWARE

In PLAXIS 2015 (3D), complex geometry of soil and structures can be defined in two different modes. These modes are defined specifically for soil or structural modeling. Independent solid models can automatically be intersected and meshed

5. HARDENING SOIL MODEL BEHAVIOR (HS)

The hardening soil model is an advanced model for the simulation of soil behavior. As for the Mohr-Coulomb model, limiting states of stress are described by means of the friction angle, ϕ, the cohesion, c, and the dilatancy angle, ψ. However, soil stiffness is described much more accurately by using three different input stiffnesses: the triaxial loading stiffness, E_{50}, the triaxial unloading stiffness, E_{ur} , and the oedometer loading stiffness, E_{oed} . As average values for various soil types, $E_{ur} \approx 3E_{50}$ and $E_{oed} \approx E_{50}$ are suggested as default settings, but both very soft and very stiff soils tend to give other ratios of E_{oed}/E_{50}, which can be defined. In contrast to the Mohr-Coulomb model, the Hardening Soil model also accounts for stress-dependency of stiffness moduli. This means that the stiffness increases with pressure. Hence, all three input stiffnesses relate to a reference stress, usually taken as 100 kPa (O'Neill, and Raines (1991).

The hardening soil model with small-strain stiffness (HS_{small}) is a modification of the above hardening soil model that accounts for the increased stiffness of soils at small strains. At low strain levels, most soils exhibit a higher stiffness than at engineering strain levels, and this stiffness varies non-linearly with strain. This behavior is described in the HS_{small} model using an additional strain-history parameter and two additional material parameters, i.e. G_0^{ref} and $\gamma_{0.7}$. G_0^{ref} is the small-strain shear modulus and $\gamma_{0.7}$ is the strain level at which the shear modulus has reduced to about 70% of the small-strain shear modulus (Iskander, 2010). The advanced features of the HS_{small} model are most apparent in working load conditions. Here, the model gives more reliable displacements than the HS model. When used in dynamic applications, the hardening soil model with small-strain stiffness also introduces hysteretic material damping

(Józsa, 2011). The hardening soil model, however, supersedes the hyperbolic model by far: Firstly by using the theory of plasticity rather than the theory of elasticity, secondly by including soil dilatancy and thirdly by introducing a yield cap. Some basic characteristics of the model are (Plaxis Manual, 2015) in Table 1:

Table 1. Hardening soil model parameters.

Stress dependent stiffness according to a power law	Input parameter m
Plastic straining due to primary deviatoric loading	Input parameter E_{50}^{ref}
Plastic straining due to primary compression	Input parameter E_{oed}^{ref}
Elastic unloading / reloading	Input parameters E_{ur}^{ref} , ν_{ur}
Failure according to the Mohr-Coulomb failure criterion	Input parameters c, ϕ and ψ

A basic feature of the present hardening soil model is the stress dependency of soil stiffness. For oedometer conditions of stress and strain, the model implies for example the relationship $E_{oed} = E_{oed}^{ref}(\sigma/p^{ref})^m$. In the special case of soft soils it is realistic to use m = 1. In such situations there is also a simple relationship between the modified compression index λ^*, as used in models for soft soil and the oedometer loading modulus in equation (5) (Plaxis Manual, 2015):

$$E_{oed}^{ref} = \frac{p^{ref}}{\lambda^*}\lambda^* = \frac{\lambda}{(1+e_0)} \tag{5}$$

Where p^{ref} is a reference pressure. Here we consider a tangent oedometer modulus at a particular reference pressure p^{ref}.

For the sake of convenience, restriction is made here to triaxial loading conditions with $\sigma'_2 = \sigma'_3$ and σ'_1 being the major compressive stress. Moreover, it is assumed that $q < q_f$, as also indicated in Fig. 2. It should also be realised that compressive stress and strain are considered negative (Schanz et al., 1999).

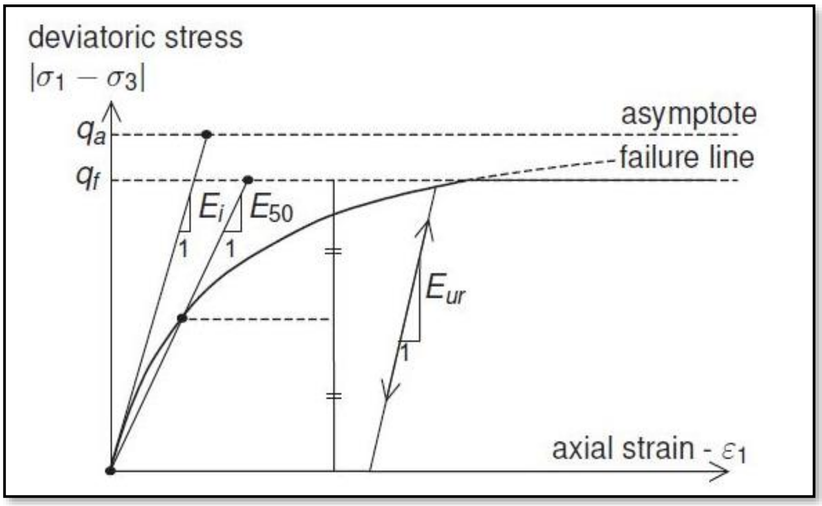

Fig. 2. Hyperbolic stress-strain relation in primary loading for a standard drained triaxial test (Atkinson and Bransby, 2012).

6. PARAMETERS OF THE (HSSMALL) MODEL

This model is, as the name indicates, a version of the hardening-soil model. Hardening-soil model with small-strain stiffness (HS small-model) is a more advanced version, with focus on describing soil's behavior more accurately while unloading and reloading the soil. The original HS-model models the stress-strain relation in this phase as linear-elastic with the stiffness E_{ur}. The HS small-model requires several parameters which are generally familiar to most geotechnical engineers. The parameters can be obtained from basic tests on soil samples, these parameters with their standard units are in Table 2.

7. CONSTRUCTION OF THE MODEL AND MESHING

In PLAXIS (2015), the geometry is defined by vertical "boreholes" and horizontal "work planes". The work planes are used to define geometry points, geometry lines, clusters, loads, boundary conditions and structures.

When creating a geometry model, it is usual to start defining the boreholes and thus the vertical depth of the model. Vertical is defined as the y-direction. The boreholes are divided in layers, which subsequently are assigned different materials (i.e. different soil properties). When multiple boreholes are present in the model, the soil properties are interpolated between the boreholes thus creating non horizontal soil layers. The pore pressure distribution is defined in the boreholes. The distribution could be entered manually (Vermeer and Brinkgreve, 2012).

Table 2. Soil parameters for HS small strain model (Likitlersuang et al., 2013).

Parameters	Symbol	Unit
Unsaturated unit weight	γ_{unsat}	kN/m^3
Saturated unit weight	γ_{sat}	kN/m^3
Secant stiffness from triaxial test at reference pressure	E_{50}^{ref}	kN/m^2
Tangent stiffness from oedometer test at pressure	E_{oed}^{ref}	kN/m^2
Unloading/reloading stiffness	E_{ur}^{ref}	kN/m^2
Power for stress- dependent stiffness	m	--
Cohesion	c'_{ref}	kN/m^2
Friction angle	$\acute{\phi}$	o
Dilatancy angle	ψ	o
Small-strain shear modulus (reference shear stiffness at small strains (HS small))	G_0^{ref}	kN/m^2
Thershold shear strain (Shear strain at which G has reduced to 70% (HS small))	$\gamma_{0.7}$	--
Poisson's ratio in unloading / reloading	$\acute{\nu}_{ur}$	--
Reference stress (100 kPa)	p_{ref}	kN/m^2
Coefficient for lateral stress under primary loading	K_0^{Nc}	--
Interface strength reduction	R_{inter}	--
Failure ratio $qf\ /qa$ like in Duncan-Chang model (0.9)	R_f	kN/m^2
Coefficient for lateral initial stress	K_0	--

8. SIMULATION OF THE EXPERIMENTAL PIPE PILE GROUP MODEL (MODEL TEST)

The pipe piles are made of aluminum, while the tested soil is Karbela sand. A group of (2x2) piles are considered here as a reference for checking the numerical solution implemented by PLAXIS-3D (2015) program. The height of sand column inside the open ended piles was represented in the numerical program as measured in the experiential work depending on the driving method, where the sand columns lengths vary from 195 mm to 295 mm as shown in Table 3. Which also presents the characteristics of the situation that was taken from the cases of experimental work of Al-Gharrawi (2016).

Table 3. Model parameters for the study of the experimental model (Al-Gharrawi, 2016).

Experimental model properties	values
Embedded pile length (mm) (L/D=15)	450
Number of piles	4
Type of pipe piles	open end piles
Pipe pile material	aluminum
Method of piles installation	driven
Spacing between piles (3d) (mm)	90 x90
State of soil	loose
Cohesion (c) (kN/m^2)	0
Angle of internal friction (°)	31
Plug condition (different soil column lengths in open pipe pile)	full plug , no symmetry configuration different soil plug length
Soil penetration depth (mm) for pile No.1 to 4 respectively as shown in Fig. 3.	216, 216, 295, 195 mm

The sand is modeled utilizing the (HS small) model, the parameters are listed in Table 4. The steel pile cap has dealt with as a linear elastic by given a modulus of elasticity and Poison´s ratio values.

Using PLAXIS-3D (2015) program, the mesh can be generated as three analyses were performed depending on the accuracy of problem: one with a coarse, one with a medium and one with a very fine mesh. For each one, 6 models are analyzed using different the interface elements. The R_{inter} coefficient values were changed from 0.1 to 1. R_{inter} factor which relates the interface strength (wall friction adhesion) to the soil strength (friction angle and cohesion).

Fig. 3 shows that mesh generation of the verification problem. Different meshes were tried from medium type to very fine depending on the accuracy parts in calculating the displacements and stiffness

Table 4. Material properties of the sand adopted soil model using hardening soil model with small strain stiffness.

Plaxis model parameters	Loose sand
Unit weight (kN/m^3)	15.5
Drainage type	Drained
$E_{50,ref}$ (kPa)	15000
$E_{oed,\ ref}$ (kPa)	15000
$E_{ur,ref}$ (kPa)	45000
m	0.625
V_{ur}	0.2
P_{ref} (kPa)	100
$\gamma_{0.7}$	0.176×10^{-3}
$G_{0,ref}$ (kPa)	75000
Cohesion c (kPa)	0.1
Friction angle (ϕ)	31
Dilatancty angle (ψ)	1
Tension cut-off (kPa)	0
R_{inter}	0.8
K_{0NC}	0.5

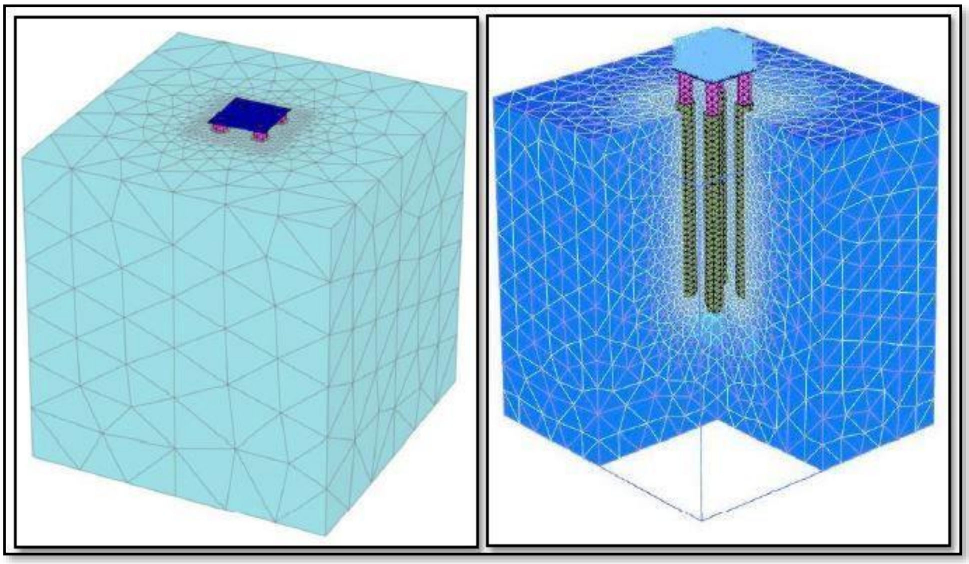

Fig. 3. Generated mesh for the verification problem.

Fig. 4 shows the problem analyzed by PLAXIS-3D program, while Fig. 5 presents the mesh and stress distribution obtained from the finite element analysis under the vertical loading, taking into account the elastic behavior of the pipe pile group and the ealastoplastic behavior of sandy soil by incorporating the hardening soil model with small strain stiffness.

Fig. 5 shows the values of vertical displacement where the maximum vertical displacement value reaches to 11.72 mm at failure in element No.15985 and node 13400 as illustrated in Fig. 5-a. Fig. 5-b shows the location of the element that has maximum displacement at the end of pile. Figs. 5-c and Fig. 5-d demonstrate the distribution of stresses along piles and the total stresses at the end bearing of piles.

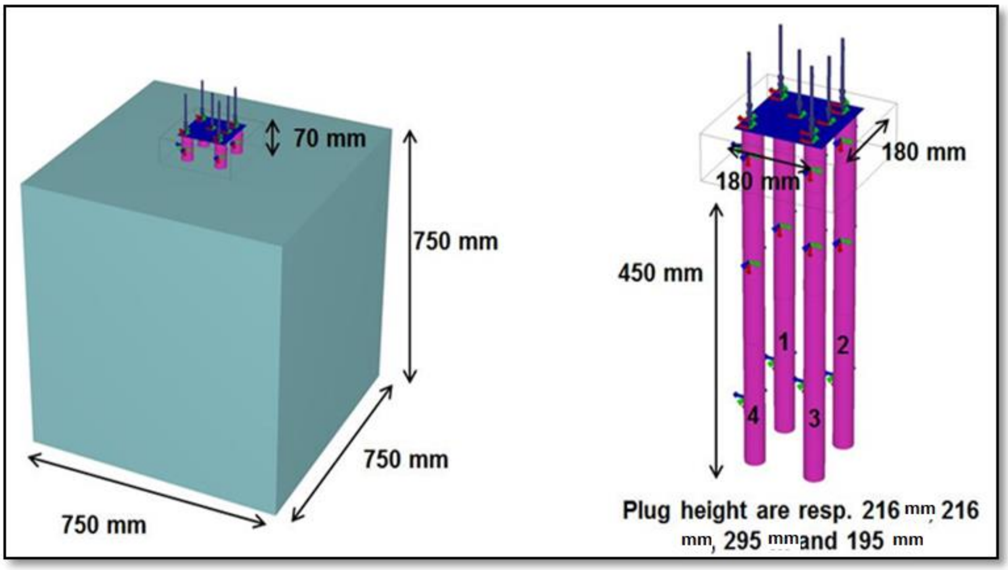

Fig. 4. Pipe pile group model G2 (2x2) with plug.

The soil stiffness and the strength model parameters have limited effects when remaining within acceptable range. It is believed that the stiffer behavior is due to installation effects that increase soil horizontal stresses and enable larger shear mobilization along the pile. This can be introduced in the model by artificially increasing the value of $K_0 ini$.

K_0 should be increased to high values ($K_0 = 2.0$) along with increasing dilatancy angle in order to obtain good matching with the experimental outcomes. Pile driving causes densification of the sand around the pile especially in loose sand. The value of K_0 is critical to the evaluation of the skin friction and is the most difficult to determine reliably because it is dependent on the stress history of the soil and the changes which take place during installation of the pile. In the case of driven piles displacement of the soil increases the horizontal soil stress from the original

K_o value. The range value of the coefficient of horizontal soil stress for driven piles K/ K_o equal to (1- 2) (Tomlinson, 2015).

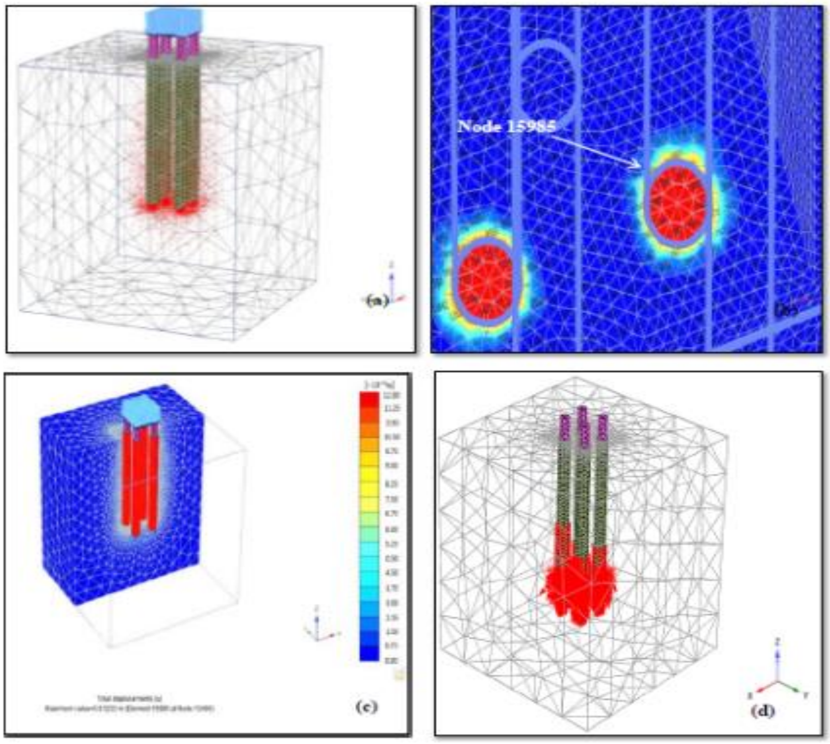

Fig. 5. Stress distribution and total displacement for pipe pile group with fully plugged state.(a) total displacement, (b) element distribution, (c) vertical stress distribution in soil plugged zone, (d) vertical stress distribution in the bearing of piles.

Fig. 6 illustrates the horizontal stress along pile with different values of lateral earth pressure. In this figure, it can be noted that the effect of driven method on the values of horizontal stresses. The horizontal stress around piles will be increased with increases depth and the maximum horizontal stresses reach to about at K equal to 2 because of the stress between soil and pile will turn into passive zone.

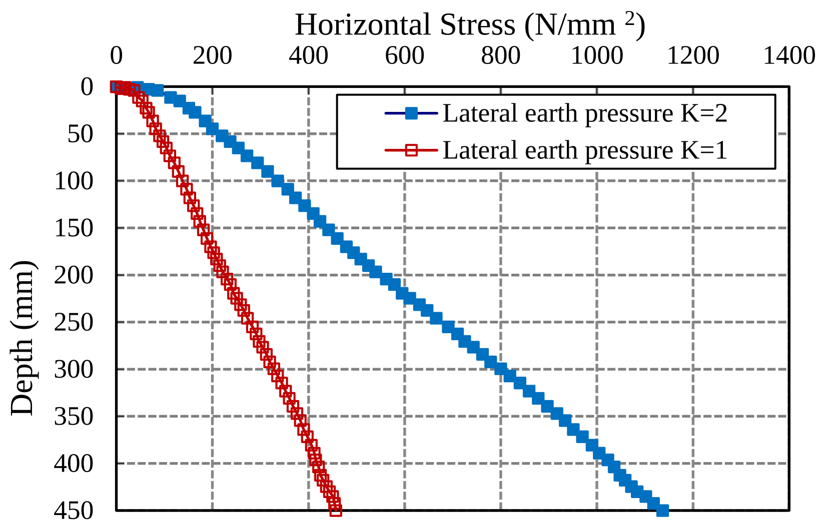

Fig. 6. Horizontal stress distribution versus depth with change of coefficient lateral earth pressure due to driven piles.

Fig. 7 shows the relationship between load-settlement curve of the theoretical and experimental work for the pile group which was tested with the number of piles and soil properties presented in Table 4.

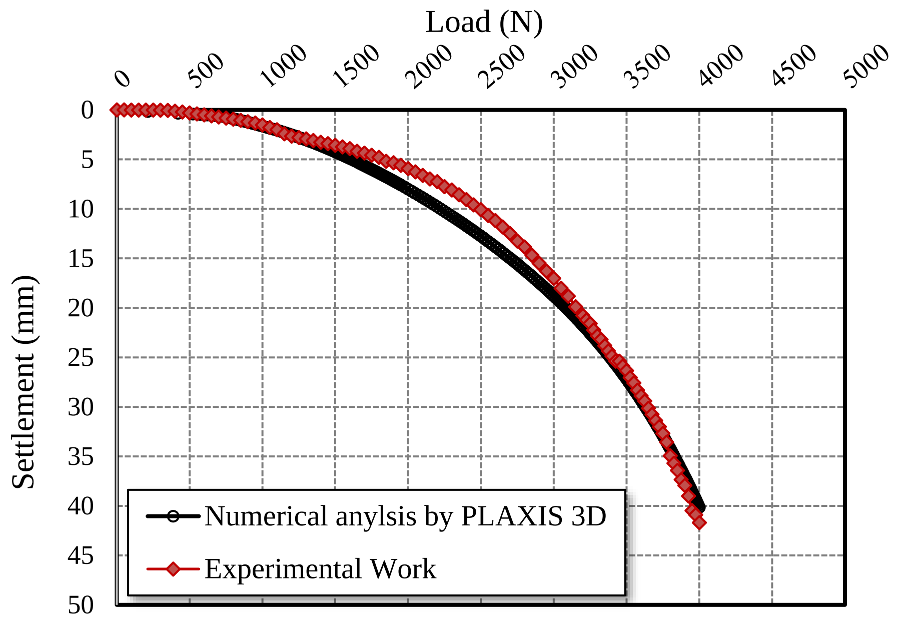

Fig. 7. Load settlement curve for 4-pipe pile groups with full plug from numerical and experiential work.

During the execution-style, driving of piles results in an increase in the density of the soil, so the value of lateral earth pressure value increases to 2. From the relationship shown in Fig. 8 and by using Plaxis-3D (2015) program, by means of finite element, and the experimental results of the model, it can be noted that the maximum percentage of error between these results is not more than 13.6 %. This is a good correlation for the results especially when the coefficient of the lateral earth pressure equals to (K_o=2). The main reason for this behavior can be attributed to the technique of pile installation and to the increment of the soil lateral pressure from the pile and the soil turned to the passive case instead of at rest condition.

The inner shaft resistance is effectively mobilized during driving due to the inertia of the soil plug. Only imperfect plugging of the pipe pile occurs during driving. In the static load test, the outer shaft resistance is predominantly mobilized at initial loading stage until it reaches the ultimate state. After the outer shat resistance is fully mobilized, the inner shaft resistance starts to mobilize.

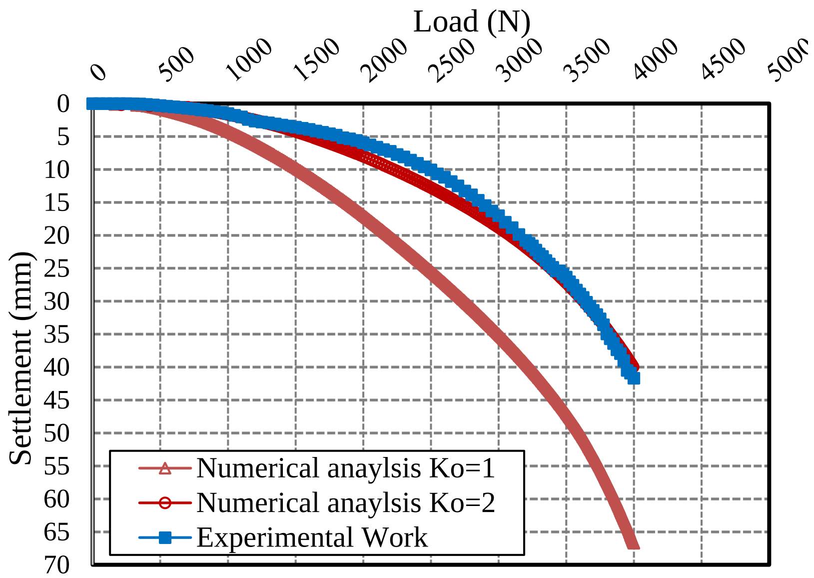

Fig. 8. Load-settlement curve showing a comparison between experimental and finite element results for case (2×2) with full plug.

9. CONCLUSIONS

1. The soil stiffness and the strength model parameters have limited effects when remaining within acceptable range.
2. Hardening soil model with small strain is considered good model to represent the case of pipe pile group and get to the convergence between experimental and theoretical results by using PLAXIS-3d program.
3. It is believed that the stiffer behavior is due to installation effect that increases the soil horizontal stresses and enables larger shear mobilization. This can be introduced in the model by theoretical increasing of the initial lateral earth pressure coefficient (K_o). The

coefficient of earth pressure should be increased to high value (2) to obtain very good match with experimental tests.

10. REFERENCES

Al-Gharrawi, A. M. B., (2016), "Load Carrying Capacity of Open and Closed Ended Pipe Pile" Ph.D. thesis, Building and Construction Engineering Department, University of Technology, Baghdad, Iraq.

American Petroleum Institute (API), (1991), “Recommended Practice for Planning, Designing and Constructing of Fixed Offshore Platforms –RP2A-LRFD,19th Edition, Washington.

Atkinson, J.H., Bransby, P.L., (2012), “The Mechanics of Soils: An Introduction to Critical State Soil Mechanics”, New York: McGraw-Hill Book Co.

Fattah, M. Y., Al-Soudani, W. H. S., (2016), "Bearing Capacity of Open-Ended Pipe Piles with Restricted Soil Plug", Ships and Offshore Structures, Vol. 11, 5, pp. 501-516, Taylor & Francis, DOI: 10.1080/17445302.2015.1030247, London W1T 3JH, UK.

Foray, P., Balachowski, L., and Colliat, J.L., (1998), “Bearing Capacity of Model Piles Driven in Dense over Consolidated Sands”, Canadian Geotechnical Journal, Vol.35, No. 2, pp. 374-385.

Iskander, M., (2010), "Behavior of Pipe Piles in Sand Plugging and Pore Water Pressure Generation during Installation and Loading", Springer Ser Geomech GeoEng.

Jardine, R. J., Overy, R. F., Chow, F. C., (1998), “Axial Capacity of Offshore Piles in Dense North Sea Sands”, Journal of Geotechnical and Geoenvironmental Engineering, ASCE, Vol. 124, No.2, pp.171-178.

Kishida, H. (1967), “The Ultimate Bearing Capacity of Pipe Piles in Sand”, Proceedings of the 3rd Asian Regional Conference of Soil Mechanics and Foundation Engineering, Vol.1, pp. 196-199.

Klos, J., and Tejchman, A., (1977), “Analysis of Behavior of Tubular Piles in Subsoil”, Proceedings of the 9thinternational conference on Soil Mechanics and Foundation Engineering, Tokyo, Vol. 1, pp. 605-608.

Likitlersuang, S., Surarak, C., Wanatowski, D., Oh, E., Balasubramaniam, A.S., (2013), “Geotechnical Parameters from Pressure Meter Tests for MRT Blue Line Extension in Bangkok”, Geomechanics and Engineering, An International Journal, Vol. 5, No. 2, pp. 99-118.

Murff, J.D., Raines, R.D., Randolph, M.F., (1990), "Soil plug behavior of piles in sand", Proceedings of the 22nd Offshore Technology conference, Houston, OTC 6421, pp.25–32.

Paikowski, S.G., Whitman, R.V., (1990), "The effect of plugging on pile performance and design", Canadian Geotechnical Journal, 24(7), pp. 429–440.

O’Neill, M.W., and Raines, R.D., (1991), “Load Transfer for Pipe Piles in Highly Pressured Dense Sand”, Journal of Geotechnical Engineering, ASCE, Vol.117, No. 8, pp. 1208-1226.

Paik, K. and Salgado, R. (2003), "Determination of bearing capacity of open-ended piles in sand”, Journal of Geotechnical and Geoenvironmental Engineering, ASCE, Vol. 129, No. 1, pp. 46 – 57.

Paik, K., Salgado, R., and Lee. J. Kim B., (2003), “Behavior of Open-and Closed-Ended Piles Driven into Sands. Journal of Geotechnical and Geoenvironmental Engineering, ASCE, Vol. 129, No. 4, pp. 296-306.

PLAXIS-3D, (2015), “Foundation Tutorial Manual”, Version 1, 2015.

Randolph, M. F., May, M., Leong, E.C., and Houlsby, G. T. (1991), “One-Dimensional Analysis of Soil Plug in Pipe Piles”, Geotechnique Vol. 41, No. 4, pp. 587-598.

Tomlinson, M.J., (2015), “Foundation Design and Construction”, 7th Edition London, Pitman.

Vermeer P. A., and Brinkgreve R. B. (2012), “PLAXIS 3D-Finite Element Code for Soil and Rocks Analysis”, Balkema, Rotterdam, the Netherlands, 2012.

White, D.J., and Bolton, M.D., (2005), “Comparing CPT and Pile Base Resistance in Sand”, Proceedings Institution of Civil Engineers, Geotechnical Engineering, Vol.158 No.1, pp.3-14.